

Resonance Raman Characterization of Highly Reduced Iron Octaethylporphyrin: $[\text{Fe}(\text{OEP})]^{n-}$ ($n = 0, 1, \text{ and } 2$)

J. Teraoka,[†] S. Hashimoto,[‡] H. Sugimoto,[†] M. Mori,[†] and T. Kitagawa*^{†‡}

Contribution from the Department of Chemistry, Faculty of Science, Osaka City University, Sugimoto-cho, Sumiyoshi-ku, Osaka, 558 Japan, and Institute for Molecular Science, Okazaki National Research Institutes, Myodaiji, Okazaki, 444 Japan. Received June 2, 1986

Abstract: Resonance Raman, EPR, and visible absorption spectra were observed for highly reduced iron-octaethylporphyrin complexes, $[\text{Fe}(\text{OEP})]^{n-}$ which were obtained in tetrahydrofuran (THF) by the sodium mirror contact reduction technique. Raman and EPR spectra were measured with the same preparation as characterized by the visible absorption spectrum which showed clear isosbestic points in each stage of the oxidoreduction: $\text{Fe}^{\text{III}}(\text{OEP})\text{Cl} \rightleftharpoons \text{Fe}^{\text{II}}(\text{OEP})(\text{THF}) \rightleftharpoons [\text{Fe}(\text{OEP})]^- \rightleftharpoons [\text{Fe}(\text{OEP})]^{2-}$. Raman lines of $[\text{Fe}(\text{OEP})]^-$ and $[\text{Fe}(\text{OEP})]^{2-}$ were qualitatively assigned on the basis of the frequency shifts observed for ^{15}N -substitution and meso-deuteriation. $[\text{Fe}(\text{OEP})]^-$ which yielded EPR signals at $g_{\perp} = 2.26$ and $g_{\parallel} = 1.93$ at 77 K but no signals at room temperature gave the ν_4 line at the same frequency as the Fe^{II} complex but the ν_{10} line at much lower frequency at room temperature. The overall spectral pattern of $[\text{Fe}(\text{OEP})]^-$ in THF was distinctly different from that of $\text{Fe}^{\text{II}}(\text{OEP})$ in THF and showed clear change upon freezing of the solution, in agreement with the reported spin transition upon freezing. Accordingly, $[\text{Fe}(\text{OEP})]^-$ in THF solution was assigned to the high-spin Fe^{I} porphyrin. $[\text{Fe}(\text{OEP})]^{2-}$, which showed a hyper type absorption spectrum and was EPR silent, gave the ν_4 line at a considerably lower frequency but the C_aC_m stretching modes at frequencies similar to those of the low-spin $\text{Fe}^{\text{I}}(\text{OEP})$ in frozen THF. The ν_4 mode of $[\text{Fe}(\text{OEP})]^{2-}$ exhibited an appreciable frequency shift upon meso-deuteriation as well as upon ^{15}N -substitution in contrast with other cases. This implied more mixing of the C_aN and C_aC_m stretching modes and thus increased π -conjugation of the two bonds. Frequencies of the modes involving the C_bC_b stretching character like ν_2 and ν_{11} were distinctly lower for $[\text{Fe}(\text{OEP})]^{2-}$, suggesting the formation of a porphyrin π -anion radical.

Importance of an electron-rich iron porphyrins have been stressed for porphyrin chemistry.¹ The first intermediate in heme catabolism is considered to be an Fe^{I} oxoporphyrin,² which is in a thermal equilibrium with Fe^{II} oxoporphyrin anion radical at room temperature.³ The molecular structures of the so called iron(I) and iron(0) tetraphenylporphyrin complexes, designated as $[\text{Fe}(\text{TPP})]^-$ and $[\text{Fe}(\text{TPP})]^{2-}$, respectively, were elucidated with X-ray crystallographic analysis,⁴ and it was pointed out that the interpretation of their structures requires inclusion of the Fe^{II} porphyrin π -anion character even in the case of $[\text{Fe}(\text{TPP})]^-$. However, so far no sign of thermal migration of the d electrons from Fe to porphyrin seems to have been obtained in the visible absorption and EPR spectroscopies of $[\text{Fe}(\text{TPP})]^-$. $[\text{Fe}(\text{TPP})]^{2-}$, which has been considered to have considerable π -anion character,⁴ has been conveniently called green species,^{1,7} but in our preliminary experiment the chemical species which is thought to correspond to this oxidation state looked brown and gave a typical hyper-type absorption spectrum. A greenish compound was generated only after this reduction stage. These apparent inconsistencies strongly suggested the necessity of reexamining the whole chemistry of highly reduced iron porphyrins from two standpoints, that is, their generation and specification. In most of the studies thus far made,⁵⁻⁷ highly reduced metalloporphyrins have been prepared by electrolytic reduction. However, electrolysis often produced undesirable byproducts, and this might have caused much of the discrepancies such as described above. In the present study, highly reduced species were generated in clean conditions by the sodium mirror contact technique. This, we believe, has removed a considerable part of the ambiguities caused by undesirable reactions.

Resonance Raman (RR) spectroscopy has been one of the most powerful tools in studies of heme proteins⁸ and metalloporphyrins.^{9,10} Some of RR lines serve as a sensitive indicator of the electronic state, the coordination number, or the core size of iron porphyrins. Among them, the ν_4 line appearing in the 1350–1375- cm^{-1} region seems to reflect the number of d_{π} electrons.^{11,12} The ferrous intermediate-spin and ferric low-spin porphyrins with the same number of d_{π} electrons (three) give rise to the ν_4 line at similar frequencies.¹³ The ferryl low-spin heme present in compound II of horseradish peroxidase having two d_{π}

electrons gives the ν_4 line at frequencies higher than the ferric hemes.^{14,15} The ν_4 frequencies of the ferrous low-spin complexes having a π acidic axial ligand such as O_2 , NO, and CO are higher than those of the σ -type ferrous low-spin complexes,^{11,12} probably due to the decrease of the effective number of the d_{π} electrons. The effect of d_{π} electrons on the ν_4 frequency might be understood if we assume that the increase in the number of the d_{π} electrons results in an increase of electrons delocalized to the porphyrin π^* orbitals ($5e_g$) which are antibonding about the C_aN bond¹⁶ and thus in a decrease of the C_aN stretching force constant which determines the ν_4 frequency.¹⁷

Reduced cytochrome P-450 gives the ν_4 line at frequencies appreciably lower than those of ferrous hemeproteins.^{18,19} This

(1) Reed, C. A. *Adv. Chem. Ser.* **1982**, 201, 333.

(2) Sano, S.; Sugiura, Y.; Maeda, Y.; Ogawa, S.; Morishima, I. *J. Am. Chem. Soc.* **1981**, 103, 2888.

(3) Sano, S.; Sano, T.; Morishima, I.; Shiro, Y.; Maeda, Y. *Proc. Natl. Acad. Sci. U.S.A.* **1985**, 83, 531.

(4) Mashiko, T.; Reed, C. A.; Haller, K. J.; Scheidt, W. R. *Inorg. Chem.* **1984**, 23, 3192.

(5) Cohen, I. A.; Ostfeld, D.; Lichtenstein, B. *J. Am. Chem. Soc.* **1972**, 94, 4522.

(6) Lexa, D.; Momenteau, M.; Mispelter, J. *Biochim. Biophys. Acta* **1974**, 338, 151.

(7) Kadish, K. M.; Larson, G.; Lexa, D.; Momenteau, M. *J. Am. Chem. Soc.* **1975**, 97, 282.

(8) Kitagawa, T.; Teraoka, J. *The Biological Chemistry of Iron*; Dunford, H. B., Dolphin, D., Raymond, K. N., Sieker, L., Eds.; D. Reidel: Dordrecht: Holland, 1982; p 375.

(9) Solovoyov, K. N.; Gladkov, L. L.; Starukhin, A. S.; Shkirman, S. F. *Spectroscopy of Porphyrins: Vibrational State*; Nauka: I Tekhnika 1985.

(10) Spiro, T. G. *Iron Porphyrins*; Lever, A. B. P., Gray, H. B., Eds.; Addison-Wesley: Reading, 1983; Vol. 2, p 91.

(11) Spiro, T. G.; Streckas, T. C. *J. Am. Chem. Soc.* **1974**, 96, 338.

(12) (a) Kitagawa, T.; Iizuka, T.; Ikeda-Saito, M.; Kyogoku, Y. *Chem. Lett.* **1975**, 849. (b) Kitagawa, T.; Kyogoku, Y.; Iizuka, T.; Ikeda-Saito, M. *J. Am. Chem. Soc.* **1976**, 98, 5169.

(13) Kitagawa, T.; Teraoka, J. *Chem. Phys. Lett.* **1979**, 63, 443.

(14) Rakhit, G.; Spiro, T. G.; Uyeda, M. *Biochem. Biophys. Res. Commun.* **1976**, 71, 803.

(15) Felton, R. H.; Romans, A. Y.; Yu, N. T.; Schonbaum, G. R. *Biochim. Biophys. Acta* **1976**, 434, 82.

(16) Kashiwagi, H.; Obara, S. *Int. J. Quant. Chem.* **1981**, 20, 843.

(17) Abe, M.; Kitagawa, T.; Kyogoku, Y. *J. Chem. Phys.* **1978**, 69, 4526.

[†] Osaka City University.

[‡] Okazaki National Research Institutes.

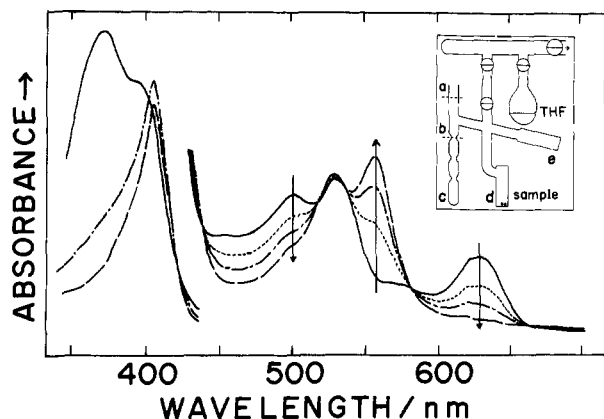


Figure 1. Changes of visible absorption spectra of $\text{Fe}^{\text{III}}(\text{OEP})\text{Cl}$ in THF upon contact with the Na mirror. Arrows denote the direction of changes upon prolonged contact. The Soret band was measured with separate preparations due to quite different optical density from that in the Q band region. The inset figure depicts the reaction compartment used. Here, a, b, and c compose the distillation tower of sodium, and d and e stand for the cells for Raman scattering and absorption spectra, respectively. For the measurements of EPR spectra, other arms were added besides the absorption cell.

could be interpreted in terms of strong π donation from the axial thiolate ligand, which should cause a secondary flow of a charge into the porphyrin ring. We are curious to know to which case such electron-rich heme belongs, the Fe^{I} porphyrin or the Fe^{II} porphyrin π -anion radical. Furthermore, since the measurements on the RR spectra of reaction intermediates of heme enzymes have become increasingly popular,²⁰ basic data on the RR spectra of reduced porphyrin are necessary for analysis of the spectra of intermediates.

Although RR spectra of porphyrin monoanion and dianion^{21,22} and of Fe^{I} porphyrin²³ were reported, there has been no isotope data, and RR spectral characterization has not always been sufficient. Therefore, we intended to measure the RR spectra of highly reduced iron-octaethylporphyrin [$\text{Fe}(\text{OEP})$] complexes in solution with the same preparation as characterized by visible absorption and EPR spectra.

Experimental Procedures

$\text{Fe}^{\text{III}}(\text{OEP})\text{Cl}$, its meso-deuteriated derivative [$\text{Fe}^{\text{III}}(\text{OEP}-d_4)\text{Cl}$], and ^{15}N -substituted one [$\text{Fe}^{\text{III}}(\text{OEP}-^{15}\text{N}_4)\text{Cl}$] were synthesized by a reported method.²⁴ To obtain the highly reduced sample in clean conditions, we adopted the sodium mirror contact reduction technique.⁶ The apparatus used is illustrated in the inset of Figure 1, in which the cell compartments (d for Raman and e for visible absorption or EPR) are not fully depicted. Solid $\text{Fe}^{\text{III}}(\text{OEP})\text{Cl}$ (or isotope derivatives) is placed in the cell d, and then the cell is connected to the system by glass blowing. After putting sodium metal to c through a, the tube is sealed at a, and the whole system is evacuated up to 10^{-5} mmHg. The solid sodium was distilled stepwise through the wave-shaped glass tube (four steps), and finally a thin layer with metallic luster (Na mirror) was formed on the glass wall between

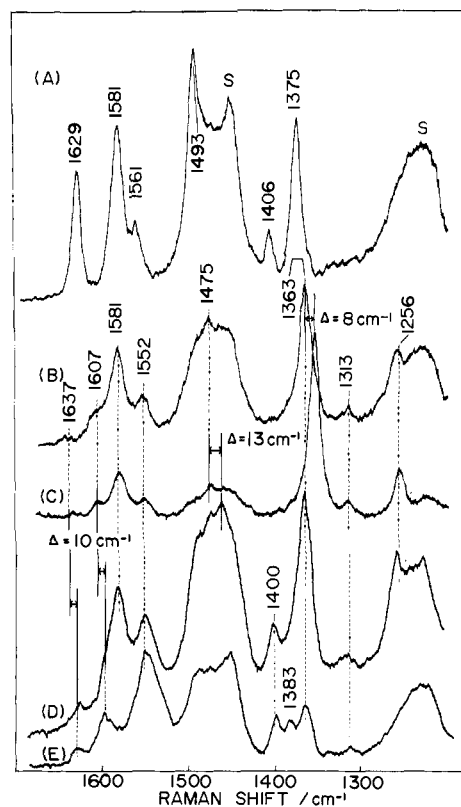


Figure 2. Resonance Raman spectra of $\text{Fe}^{\text{III}}(\text{OEP})\text{Cl}$ (A), $\text{Fe}^{\text{II}}(\text{OEP})$ (B), $\text{Fe}^{\text{II}}(\text{OEP}-^{15}\text{N}_4)$ (C), and $\text{Fe}^{\text{II}}(\text{OEP}-d_4)$ (D and E) all in the THF solution. The Raman lines marked by S are due to solvent. Experimental conditions (A–D): laser, 441.6 nm, 40 mW; sensitivity, 1000 counts/s; scan speed, 25 $\text{cm}^{-1}/\text{min}$; slit width, 5 cm^{-1} ; time constant, 1.6 s; (E): laser 514.5 nm, 70 mW; sensitivity, 2500 counts/s; scan speed, 25 $\text{cm}^{-1}/\text{min}$; slit width, 6 cm^{-1} ; time constant, 3.2 s.

a and b, and the tube was sealed at b. Thoroughly degassed and dehydrated tetrahydrofuran (THF)²⁵ was distilled into d, and the reaction compartment was sealed and detached from the vacuum line.

The THF solution of $\text{Fe}^{\text{III}}(\text{OEP})\text{Cl}$ in d was brought into contact with the Na mirror by tipping the apparatus, and there the solution was slightly shaken for a required time. The resultant solution was brought back to d for measurement of Raman spectra and to e for measurement of EPR or visible absorption spectra. The solution was returned to the Na mirror for more reduction, and the measurements were repeated. In this way different kinds of spectra were measured with the same preparation.

Raman scattering was excited by a He/Cd laser (Kinmon Electrics, CDR80SG) or an Ar^+ ion laser (NEC GLG3200) and recorded on a JEOL 400D Raman spectrometer, which was calibrated with indene.²⁶ Visible absorption spectra were measured with a Hitachi 220S spectrophotometer by using a 1-mm pathlength cuvette. The EPR spectra were measured at 300 and 77 K with a Varian E112 EPR spectrometer. The low-temperature measurements were carried out by installing the cells (d and e) to homemade cryostat after detaching them from the reaction compartment.

Results

Figure 1 shows changes in absorption spectra of $\text{Fe}^{\text{III}}(\text{OEP})\text{Cl}$ upon contact with the Na mirror. As an accumulated time of the contact increases, the absorption bands at 502 and 630 nm became weaker, and a new band grew at 558 nm, while the band at 529 nm remained almost unaltered. Since there are well-defined isosbestic points at 439, 518, 537, 582, and 665 nm, the spectral changes should arise from a population change of two redox components. The final spectrum at this stage was very similar to that obtained by electrochemical reduction with $E_{1/2} = -1.1$ V²⁷ and also to that of $\text{Fe}^{\text{II}}(\text{OEP})(2\text{-MeIm})$ (2-MeIm: 2-

(18) (a) Champion, P. M.; Gunsalus, I. C. *J. Am. Chem. Soc.* **1977**, *99*, 2001. (b) Champion, P. M.; Gunsalus, I. C.; Wagner, G. C. *J. Am. Chem. Soc.* **1978**, *100*, 3743.

(19) (a) Ozaki, Y.; Kitagawa, T.; Kyogoku, Y.; Shimada, H.; Iizuka, T.; Ishimura, Y. *J. Biochem. (Tokyo)* **1976**, *80*, 1447. (b) Ozaki, Y.; Kitagawa, T.; Kyogoku, Y.; Imai, Y.; Hashimoto-Yutsudo, C.; Sato, R. *Biochemistry* **1978**, *17*, 5826. (c) Shimizu, T.; Kitagawa, T.; Mitani, F.; Iizuka, T.; Ishimura, Y. *Biochim. Biophys. Acta* **1981**, *670*, 236.

(20) Kitagawa, T. In *Spectroscopy of Biological Systems*; Clark, R. J. H.; Hester, R. E.; Eds.; Advances in Spectroscopy 13; Wiley: New York, 1986; p 443.

(21) Ksenofontova, N. M.; Maslov, V. G.; Sidorov, A. N.; Bobovich, Y. S. *Opt. Spectrosc.* **1976**, *40*, 809.

(22) Yamaguchi, H.; Soeta, A.; Toeda, H.; Ito, K. *J. Electroanal. Chem.* **1983**, *159*, 347.

(23) Srivatsa, G. S.; Sawyer, D. T.; Boldt, N. J.; Bocian, D. F. *Inorg. Chem.* **1985**, *24*, 2123.

(24) Ogoshi, H.; Masai, N.; Yoshida, Z.; Takemoto, J.; Nakamoto, K. *Bull. Chem. Soc. Jpn.* **1971**, *44*, 49.

(25) In order to dehydrate THF completely, THF was kept with Na metal under 10^{-5} mmHg for a week.

(26) Hendra, P. J.; Loader, E. J. *Chem. Ind. (London)* **1968**, 718.

methylimidazole) in CH_2Cl_2 , the five-coordinate ferrous high-spin complex, reported previously.¹³ This reduced species was EPR silent.

In Figure 2 is shown the RR spectrum (B) of the sample which gave the last absorption spectrum in Figure 1, together with the spectra of the ^{15}N -substituted (C) and meso-deuteriated (D) derivatives. The RR spectrum of the starting material is also shown at the top (A). The isotopic substitutions were confirmed for the RR spectra of the starting ferric porphyrin (not shown). The Raman lines of the reduced species at 1637 and 1607 cm^{-1} , which were more clearly observed upon excitation at 514.5 nm as shown by spectrum (E) for the meso-deuteriated species, exhibited frequency shifts of -10 cm^{-1} upon meso-deuteriation but no shift upon ^{15}N substitution. Accordingly, they are assigned to the ν_{10} mode.¹⁷

On the basis of the empirical relation for the ν_{10} frequencies and the coordination number of the iron ion,^{11-13,28,29} the 1637- and 1607- cm^{-1} lines are categorized to the four-coordinate intermediate-spin and the five-coordinate high-spin states of ferrous porphyrins, respectively. Therefore, the two forms may be coexistent in the THF solution. It is noted, however, that the pure ferrous intermediate-spin complex provides much more intense ν_{10} line upon excitation at 514.5 nm,¹³ and, therefore, its low intensity in Figure 2 suggests that the equilibrium is biased to the high-spin species. The Raman line of the ferrous species at 1475 cm^{-1} appears to shift by -13 cm^{-1} upon meso-deuteriation and is accordingly assigned to the ν_3 mode, although the band center is not always clear due to overlapping with a strong solvent band.

The Raman line of the ferrous species at 1363 cm^{-1} exhibits a frequency shift of -8 cm^{-1} upon ^{15}N substitution but no shift upon meso-deuteriation. Accordingly, this line is assigned to the ν_4 mode. The RR spectra of ferrous octaethylchlorin complexes $[\text{Fe}(\text{OEC})]$ exhibit two bands in the ν_4 region,³⁰ and the number of Raman lines is generally larger for $\text{Fe}(\text{OEC})$ than for $\text{Fe}(\text{OEP})$. The singlet feature of the ν_4 band in Figure 2 and the fact that the similar number of Raman lines are observed between $\text{Fe}^{\text{II}}(\text{OEP})\text{Cl}$ and its reduced species strongly suggest that reduction of the porphyrin ring does not occur during the contact with the Na mirror. The RR spectrum of the ferrous species is close to that of $\text{Fe}^{\text{II}}(\text{OEP})(2\text{-MeIm})$ in CH_2Cl_2 prepared by a different method,¹³ and the frequencies of the marker lines such as ν_{10} and ν_3 are within the category of five-coordinate ferrous high-spin complexes. Although the X-ray crystallographic analysis on the THF complex of ferrous porphyrin³¹ demonstrated the six-coordinate structure, $\text{Fe}^{\text{II}}(\text{TPP})(\text{THF})_2$, for the solid state, the Raman data strongly suggest that the main component of the $\text{Fe}^{\text{II}}(\text{OEP})\text{-THF}$ complex in the THF solution should adopt the five-coordinate structure designated as $\text{Fe}^{\text{II}}(\text{OEP})(\text{THF})$.

Figure 3A displays changes of the absorption spectra in the Soret region upon further contact with the Na mirror. The first spectrum in Figure 3A is the same as the last spectrum of Figure 1. The absorption intensity at 407 nm gradually decreased, and new bands at 373 and 455 nm grew with isosbestic points at 378 and 427 nm. The final spectrum at this stage resembled the spectrum of the so called B form of $[\text{Fe}(\text{TPP})]^-$ in the dimethylformamide (DMF) solution⁶ and accordingly is considered to be due to $[\text{Fe}(\text{OEP})]^-$. The RR spectrum of the species, which gave the last spectrum of Figure 3A, is shown in Figure 4, where the EPR spectrum observed at 77 K is also depicted in the inset.

(27) The previously reported spectrum of $\text{Fe}^{\text{II}}(\text{OEP})$ in THF solution obtained from $\text{Fe}^{\text{II}}(\text{OEP})(\text{Py})_2$ is similar to the spectrum of electrochemically reduced molecule with $E_{1/2} = -0.36 \text{ V}$ but is different from the spectrum shown in Figure 1. The spectra of the electrochemically reduced molecules were communicated by Prof. H. Ogoshi of Nagaoka Science and Engineering University.

(28) Spiro, T. G.; Stong, J. D.; Stein, P. *J. Am. Chem. Soc.* **1979**, *101*, 2648.

(29) Teraoka, J.; Kitagawa, T. *J. Phys. Chem.* **1980**, *84*, 1928.

(30) Ozaki, Y.; Iriyama, K.; Ogoshi, H.; Ochiai, T.; Kitagawa, T. *J. Phys. Chem.*, in press.

(31) Reed, C. A.; Mashiko, T.; Scheidt, W. R.; Spartalian, K.; Lang, G. *J. Am. Chem. Soc.* **1980**, *102*, 2302.

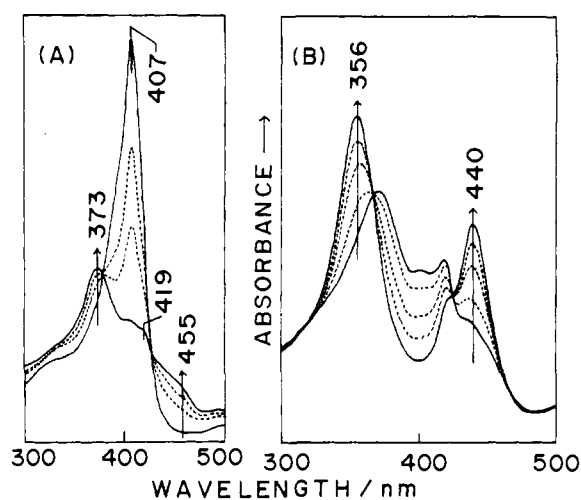


Figure 3. (A) Changes of absorption spectrum in the Soret region upon reduction from $\text{Fe}^{\text{II}}(\text{OEP})\text{-THF}$ complex to $[\text{Fe}(\text{OEP})]^-$ in THF. (B) Changes of absorption spectrum in the Soret region upon reduction from $[\text{Fe}(\text{OEP})]^-$ to $[\text{Fe}(\text{OEP})]^{2-}$ in THF.

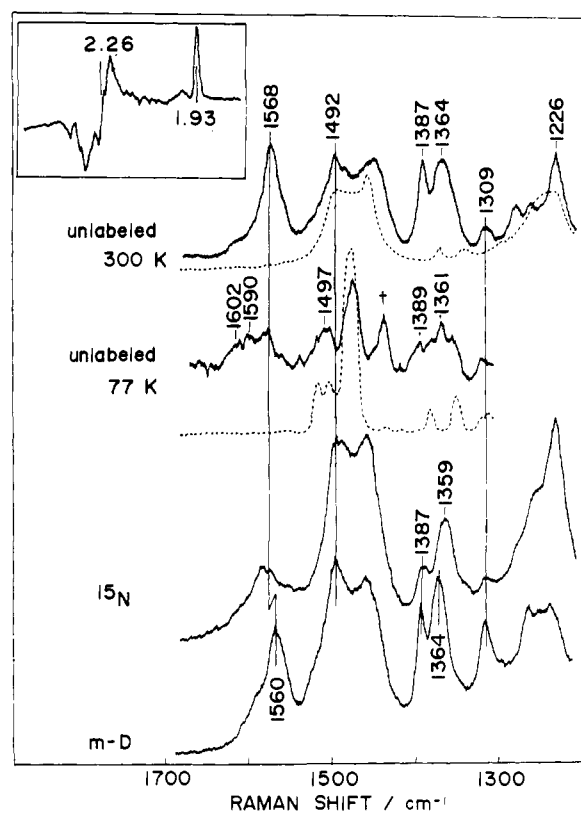


Figure 4. Resonance Raman spectra of $[\text{Fe}(\text{OEP})]^-$ at room temperature (top), $[\text{Fe}(\text{OEP})]^-$ at 77 K (second), $[\text{Fe}(\text{OEP-}^{15}\text{N}_4)]^-$ (third), and $[\text{Fe}(\text{OEP-d}_4)]^-$ (bottom). The broken lines indicate the Raman spectra of pure solvent (THF) at room temperature and 77 K. The ν_3 mode of $[\text{Fe}(\text{OEP})]^-$ contributes to the peak at 1492 cm^{-1} , but its isotope shifts are obscured due to the strong band of the solvent. The Raman line of $[\text{Fe}(\text{OEP-}^{15}\text{N}_4)]^-$ at 1580 cm^{-1} is due to contaminated Fe^{II} species (excitation, 441.6 nm). The inset shows the EPR spectrum (77 K) of the preparation used to measure the Raman spectrum (top).

This EPR spectrum gives peaks at $g_{\perp} = 2.26$ and $g_{\parallel} = 1.93$, indicating the formation of the Fe^{I} porphyrin, which is expected to yield the EPR signals of $g_{\perp} = 2.30$ and $g_{\parallel} = 1.93$.⁵ The EPR signals disappeared upon raising the temperature to 300 K but were restored upon recooling to 77 K.

The RR spectrum of this THF solution of $[\text{Fe}(\text{OEP})]^-$ at 77 K is also shown in Figure 4, where the spectra of solvent at two temperatures are shown by broken lines. Upon freezing the

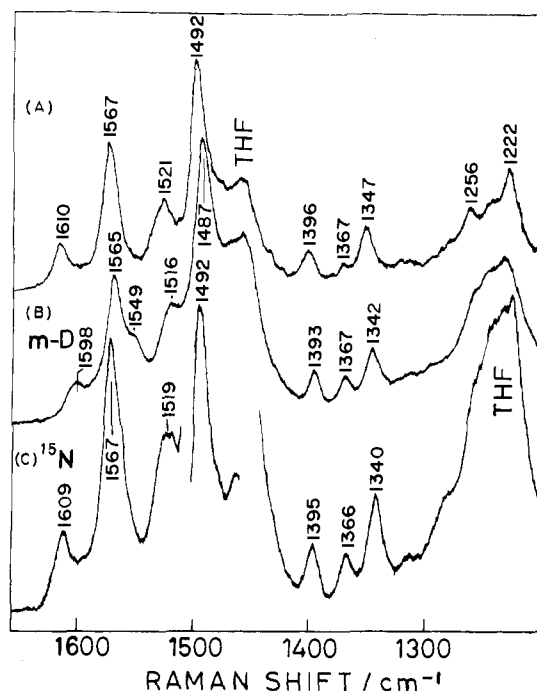


Figure 5. Resonance Raman spectra of $[\text{Fe}(\text{OEP})]^{2-}$ (A), $[\text{Fe}(\text{OEP-d}_4)]^{2-}$ (B), and $[\text{Fe}(\text{OEP-}^{15}\text{N}_4)]^{2-}$ (C) in THF solution (excitation, 441.6 nm).

solution the Raman lines at 1568, 1387, and ~ 1492 cm^{-1} became weaker, but new lines appeared at 1602, 1590, and 1497 cm^{-1} . Upon raising the temperature the original spectrum was restored. Since the spectrum of THF itself exhibits a large change upon freezing particularly in the 1450–1500- cm^{-1} region, the spectral change of $[\text{Fe}(\text{OEP})]^-$ in this frequency region cannot be clearly described. However, this large spectral change upon freezing seems compatible with the spin transition from high- to low-spin states reported by Cohen et al.⁵ These facts suggest that the RR spectra at room temperature arise from the high-spin species of $[\text{Fe}(\text{OEP})]^-$.

In the RR spectra of $[\text{Fe}(\text{OEP})]^-$ observed at room temperature, the 1364- cm^{-1} line shows a shift of -5 cm^{-1} for ^{15}N substitution but no shift for meso-deuteration and is therefore assigned to the ν_4 mode. The ν_4 frequency is almost the same as that of the Fe^{II} high-spin species shown in Figure 2. However, it is to be emphasized that the overall spectral patterns are quite different between the high-spin $\text{Fe}^{\text{II}}(\text{OEP})$ and $[\text{Fe}(\text{OEP})]^-$ both in THF, although they are reported to be quite alike for the DMF solution.²³ On the other hand, the 1568- cm^{-1} line of $[\text{Fe}(\text{OEP})]^-$ exhibits a frequency shift of -8 cm^{-1} upon meso-deuteration like the 1607- cm^{-1} line of $\text{Fe}^{\text{II}}(\text{OEP})(\text{THF})$ and is therefore assignable to the ν_{10} mode. This means that the ν_{10} mode is shifted to a considerably lower frequency (37 cm^{-1}) with the change of $\text{Fe}^{\text{II}}(\text{OEP})(\text{THF}) \rightarrow [\text{Fe}(\text{OEP})]^-$. Since the ν_{10} frequency generally becomes lower upon expansion of porphyrin core size,^{28,32} the shifted ν_{10} line may indicate the expanded porphyrin core. An alternative interpretation is to assume ruffling of the porphyrin ring which would probably cause low frequency shift of the C_aC_m stretching modes and contraction of the Fe–N bonds. $[\text{Fe}(\text{OEP})]^-$ did not give a well-defined RR spectrum upon excitation at longer wavelengths.

When $[\text{Fe}(\text{OEP})]^-$ in the THF solution was again brought into contact with the Na mirror, the absorption spectra changed with isobestic points at 366 and 427 nm as shown in Figure 3B where the first spectrum of Figure 3B is the same as the last spectrum of Figure 3A. New well-defined bands grew at 356 and 440 nm, and the spectral pattern assumed a typical hyper type. A similar

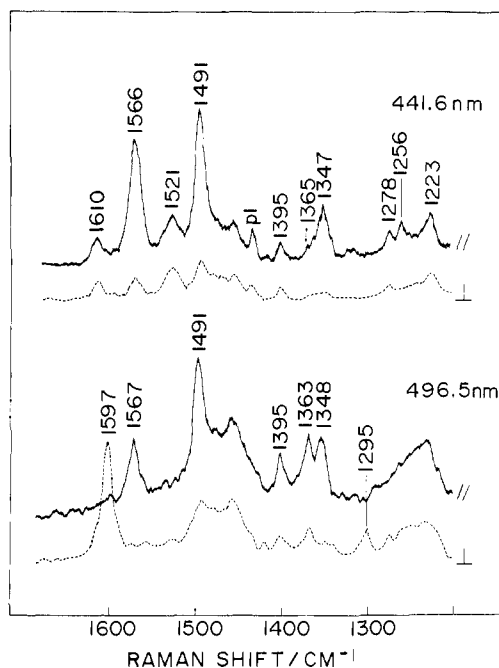


Figure 6. Polarized resonance Raman spectra of $[\text{Fe}(\text{OEP})]^{2-}$ in THF excited at 441.6 nm (upper) and at 496.5 nm (lower). Solid and broken lines denote the parallel and perpendicular components, respectively.

spectrum was previously reported for $[\text{Fe}(\text{TPP})]^{2-}$, the absorption maxima of which in the DMF solution were reported at 360 and 448 nm.⁶ In accord, the species having the absorption maxima at 356 and 440 nm, is assigned to $[\text{Fe}(\text{OEP})]^{2-}$. It is noted that this species looks apparently brown in contrast with its name of green complex. A greenish compound with the Soret band at 460 nm was obtained after further prolonged contact of $[\text{Fe}(\text{OEP})]^{2-}$ with the Na mirror.

The RR spectra of $[\text{Fe}(\text{OEP})]^{2-}$ are shown in Figure 5. The Raman line at 1347 cm^{-1} (p) exhibits a frequency shift of -7 cm^{-1} upon ^{15}N -substitution and is assigned to the ν_4 -like mode. However, this line is appreciably shifted upon meso-deuteration, suggesting a change of vibrational mode from the ordinary ν_4 mode. On the other hand, the Raman line at 1610 (dp), 1521 (dp), 1492 (p), and 1396 (dp) cm^{-1} show frequency shifts of -12 , -5 , -5 , and -3 cm^{-1} , respectively, upon meso-deuteration and are probably assignable to the ν_{10} , ν_{11} , ν_3 , and ν_{28} -like modes, respectively. They should involve the C_aC_m stretching character, the contribution of which reflects the amount of the observed shifts. Since the 1567- cm^{-1} line (p) is insensitive to both ^{15}N -substitution and meso-deuteration, this band presumably arises from the C_bC_b stretching vibration like ν_2 . Although the same mode numbers as those of the neutral porphyrin ring are used, appreciable shifts of the ν_4 and ν_{11} lines observed upon meso-deuteration of $[\text{Fe}(\text{OEP})]^{2-}$ imply a change of vibrational modes from the neutral species.

The polarized spectra of $[\text{Fe}(\text{OEP})]^{2-}$ excited at 441.6 and 496.5 nm are displayed in Figure 6. Two anomalously polarized lines are clearly observed at 1597 and 1295 cm^{-1} , which are assigned without doubt to the ν_{19} (C_aC_m stretching) and ν_{21} ($\text{C}_m\text{--H}$ in-plane bending) modes, respectively. It is unexpected that the ν_{10} line is not resonance enhanced upon excitation at 496.5 nm. On the basis of these assignments it can be concluded for $[\text{Fe}(\text{OEP})]^{2-}$ that the frequencies of the modes involving the C_bC_b stretching character like ν_2 and ν_{11} and the mode involving the C_aN stretching character like ν_4 are significantly lower than those of the Fe^{II} porphyrin, but those involving the C_aC_m stretching and $\text{C}_m\text{--H}$ bending characters are relatively unaltered.

Discussion

So far the highly reduced porphyrins have been generated mainly by electrolytic reduction, and description of $[\text{Fe}(\text{TPP})]^-$ has been somewhat controversial. From the consecutive optical

(32) (a) Felton, R. H.; Yu, N. T.; O'Shea, D. C.; Shelnut, J. A. *J. Am. Chem. Soc.* **1974**, *96*, 3675. (b) Spaulding, L. D.; Chang, C. C.; Yu, N. T.; Felton, R. H. *J. Am. Chem. Soc.* **1975**, *97*, 2517.

spectra recorded during the controlled potential electrolysis, Lexa et al.⁶ pointed out the appearance of two forms in succession for $[\text{Fe}(\text{OEP})]^-$ and the spectra are independent of the nature of axial ligands initially present. Kadish et al.⁷ confirmed this, reporting the absorption maxima at 457 and 362 nm for form A and at 420 and 390 nm for form B. Cohen et al.⁵ found from the magnetic measurements that $\text{Fe}^{\text{I}}(\text{TPP})$ assumes a single species with a high-spin state ($S = 3/2$) in the THF solution at 200–300 K but changes to the low-spin state in frozen THF. Mashiko et al.⁴ pointed out that reduction of $[\text{Fe}(\text{TPP})]^-$ produces a green species.

The present method has provided each oxidoreductive species in fairly pure form, and accordingly the visible absorption spectrum showed clearly isosbestic points in each stage of the oxidoreduction; $\text{Fe}^{\text{III}}(\text{OEP})\text{Cl} \rightleftharpoons \text{Fe}^{\text{II}}(\text{OEP})(\text{THF}) \rightleftharpoons [\text{Fe}(\text{OEP})]^- \rightleftharpoons [\text{Fe}(\text{OEP})]^{2-}$. So long as THF is thoroughly dehydrated, these spectral changes are very reproducible. The Raman and EPR spectra were observed for the species defined by the visible absorption spectra. The presence of the isosbestic points upon conversion from $\text{Fe}^{\text{II}}(\text{OEP})(\text{THF})$ to $[\text{Fe}(\text{OEP})]^-$ shown in Figure 3A suggests the appearance of one form for $[\text{Fe}(\text{OEP})]^-$ which corresponds to form B on the DMF solution;⁶ form A could not be identified for $[\text{Fe}(\text{OEP})]^-$ in THF solution. The EPR spectrum of $[\text{Fe}(\text{OEP})]^-$ shown in the inset of Figure 4 suggests the low-spin Fe^{I} porphyrin with axial symmetry. Consequently, it seems most reasonable to represent $[\text{Fe}(\text{OEP})]^-$ as $\text{Fe}^{\text{I}}(\text{OEP})$. Disappearance of EPR signals at room temperature is also compatible with the spin transition, although the intensity of the EPR signals depends on the relaxation time and accordingly the intensity alone cannot prove the spin transition. The large RR spectral changes of $[\text{Fe}(\text{OEP})]^-$ in THF upon freezing are consistent with the spin transition pointed out by Cohen et al.⁵

Srivatsa et al.²³ recently reported that frequencies of all Raman lines of $[\text{Fe}(\text{TPP})]^-$ in DMF are identical with those of $\text{Fe}^{\text{II}}(\text{TPP})$ within 2 cm^{-1} , attributing it to the formation of the Fe^{I} porphyrin instead of Fe^{II} porphyrin π -anion radical. In contrast, comparison between Figures 2(B–D) and 4 indicates that the band positions and the magnitudes of the isotope shifts are definitely different between $\text{Fe}^{\text{I}}(\text{OEP})$ and $\text{Fe}^{\text{II}}(\text{OEP})$ in the THF solution. Since DMF cannot be used for the Na mirror experiment, we failed to elucidate the origin of the discrepancy between Srivatsa et al. and the present results. We deduce that the Raman spectral difference between the Fe^{II} and Fe^{I} states within the low-spin state is much smaller than that within the high-spin state and the Raman spectral difference between the high- and low-spin states of Fe^{I} porphyrin is significantly large. The latter is based on the large shift of the ν_{10} line of $[\text{Fe}(\text{OEP})]^-$ upon freezing of THF. The compounds that Srivatsa et al. have treated might be low-spin species both in the Fe^{II} and Fe^{I} states.

One may argue against the assignment of the 1568-cm^{-1} line of $\text{Fe}^{\text{I}}(\text{OEP})$ in THF solution to ν_{10} . Indeed this frequency is unexpectedly low. Since it exhibits a frequency shift upon meso-deuteration, the Raman line should evidently involve the C_aC_m stretching character. There are four Raman active C_aC_m stretching modes: $\nu_{10} > \nu_{19} > \nu_3 > \nu_{28}$.¹⁷ Probably the order of frequencies would not be altered by a change of the oxidation state of the Fe ion. If the Raman line in question were ν_{19} , the amount of the frequency shift would be reasonable, but actually the Raman line is polarized and cannot be assigned to the A_{2g} mode. Since the ν_3 line was observed at 1497 cm^{-1} for the frozen solution and around 1492 cm^{-1} for the solution (Figure 4), the 1568-cm^{-1} line cannot be ν_3 and ν_{28} . Therefore, its assignment to ν_{10} seems most likely.

The C_aC_m stretching frequency is very sensitive to core expansion;^{28,32} the larger the core size is, the lower the C_aC_m stretching frequency is. Accordingly, the unusually low frequency of ν_{10} for the high spin $\text{Fe}^{\text{I}}(\text{OEP})$ may suggest occupation of an extra electron in the $d_{x^2-y^2}$ orbital of iron. This need not be

accompanied by a change of the C_aN bond which determines the ν_4 frequency.

It is stressed that the Fe^{I} porphyrin is quite different from the electron-rich heme of reduced cytochrome P-450; the latter gave the ν_4 line at distinctly lower frequency, but the former gave it at almost the same frequency as the Fe^{II} porphyrin. On the other hand, the P-450 model compound having a thiolate anion at the fifth coordination position did not give the ν_4 band at the unusually low frequency.³³ Therefore, the heme of reduced cytochrome P-450 might have π -anion character rather than the Fe^{I} porphyrin character.

The RR spectral characteristics of $[\text{Fe}(\text{OEP})]^{2-}$ is noteworthy. The ν_4 frequency (1347 cm^{-1}) is considerably lower than that of any high- and low-spin complexes of $\text{Fe}^{\text{II}}(\text{OEP})$ and $\text{Fe}^{\text{I}}(\text{OEP})$. The ν_4 line of metalloporphyrins usually shows frequency shifts by $5\text{--}6\text{ cm}^{-1}$ upon ^{15}N -substitution³⁴ but by $0\text{--}1\text{ cm}^{-1}$ upon meso-deuteration.³⁵ This property is not changed by the coordination number and the spin state of the Fe ion. Nonetheless, the ν_4 line of $[\text{Fe}(\text{OEP})]^{2-}$ exhibited a shift of 5 cm^{-1} upon meso-deuteration besides the shift of 7 cm^{-1} upon ^{15}N -substitution. On the other hand, normal coordinate calculation on $\text{Ni}(\text{OEP})$ predicted the shifts of 9 and 5 cm^{-1} for ^{15}N -substitution and meso-deuteration, respectively.¹⁷ Accordingly, the results on $[\text{Fe}(\text{OEP})]^{2-}$ are closer to the calculated results than those on other $\text{Fe}(\text{OEP})$ complexes. This means that the C_aC_m stretching mode is more mixed with the C_aN stretching mode for $[\text{Fe}(\text{OEP})]^{2-}$ than for other porphyrins. Presumably, the π -conjugation increased in $[\text{Fe}(\text{OEP})]^{2-}$, and as a result, the coupling constant between the C_aN and C_aC_m stretching coordinate became larger than other derivatives.

The ν_{10} and ν_3 frequencies of $[\text{Fe}(\text{OEP})]^{2-}$ (1610 and 1492 cm^{-1} , respectively) are relatively close to those of the low-spin $\text{Fe}^{\text{I}}(\text{OEP})$ (1602 and 1497 cm^{-1}). According to the X-ray crystallographic analysis,⁴ changes in bond length upon the change from $[\text{Fe}(\text{TPP})]^-$ to $[\text{Fe}(\text{TPP})]^{2-}$ are as follows: elongated from 1.401 to 1.409 \AA for C_aN and from 1.338 to 1.352 \AA for C_bC_b whereas contracted from 1.385 to 1.380 \AA for C_aC_m and from 1.429 to 1.421 \AA for C_aC_b . The fact that the change in the C_aC_m bond length is the smallest is compatible with the relatively small shifts of the ν_{10} and ν_3 modes. The appreciable stretch of the C_aN bond is in qualitative agreement with the low frequency shift of the ν_4 mode. Furthermore, the largest elongation of the C_bC_b bond is consistent with significant lowering of the Raman lines associated with the C_bC_b stretching vibrations.

It is also noted that the present results appear qualitatively consistent with the trend observed for the vanadium etioporphyrin $[\text{VO}(\text{EP})]^{2-}$,²¹ in which the C_aC_m stretching frequencies of $[\text{VO}(\text{EP})]^{0-}$ and $[\text{VO}(\text{EP})]^{2-}$ are alike but that of $[\text{VO}(\text{EP})]^-$ is lower, while the N-C_a stretching frequencies of $[\text{VO}(\text{EP})]^{0-}$ and $[\text{VO}(\text{EP})]^-$ are alike but that of $[\text{VO}(\text{EP})]^{2-}$ is lower. Since there is no X-ray data for a high-spin Fe^{I} porphyrin, the unusually low frequency of the ν_{10} mode for $\text{Fe}^{\text{I}}(\text{OEP})$ in THF solution cannot be discussed in relation to the molecular structure. The present Raman study suggests the elongated C_aC_m bond and unaltered C_aN bond for the high-spin $\text{Fe}^{\text{I}}(\text{OEP})$ compared with those for the high-spin $\text{Fe}^{\text{II}}(\text{OEP})$.

Acknowledgment. We thank Dr. T. Takui of Osaka City University for stimulating discussion on the EPR spectrum.

Registry No. $\text{Fe}(\text{OEP})^-$, 63455-43-6; $[\text{Fe}(\text{OEP})]^{2-}$, 105162-67-2; $\text{Fe}^{\text{III}}(\text{OEP})\text{Cl}$, 28755-93-3; $\text{Fe}^{\text{II}}(\text{OEP})$, 61085-06-1.

(33) Chottard, G.; Schappacher, M.; Ricard, L.; Weiss, R. *Inorg. Chem.* **1984**, *23*, 4557.

(34) Kitagawa, T.; Abe, M.; Kyogoku, Y.; Ogoshi, H.; Sugimoto, H.; Yoshida, Z. *Chem. Phys. Lett.* **1977**, *48*, 55.

(35) Kitagawa, T.; Ogoshi, H.; Watanabe, E.; Yoshida, Z. *Chem. Phys. Lett.* **1975**, *30*, 451.